



Cellulose nanocrystals modification by grafting from ring opening polymerization of a cyclic carbonate

Michaël Lalanne-Tisné, Samuel Eyley, Julien de Winter, Audrey Huret, Wim Thielemans, Philippe Zinck

► To cite this version:

Michaël Lalanne-Tisné, Samuel Eyley, Julien de Winter, Audrey Huret, Wim Thielemans, et al.. Cellulose nanocrystals modification by grafting from ring opening polymerization of a cyclic carbonate. Carbohydrate Polymers, 2022, Carbohydrate Polymers, 295, pp.119840. 10.1016/j.carbpol.2022.119840 . hal-03759014

HAL Id: hal-03759014

<https://hal.univ-lille.fr/hal-03759014>

Submitted on 21 Nov 2023

HAL is a multi-disciplinary open access archive for the deposit and dissemination of scientific research documents, whether they are published or not. The documents may come from teaching and research institutions in France or abroad, or from public or private research centers.

L'archive ouverte pluridisciplinaire **HAL**, est destinée au dépôt et à la diffusion de documents scientifiques de niveau recherche, publiés ou non, émanant des établissements d'enseignement et de recherche français ou étrangers, des laboratoires publics ou privés.



Distributed under a Creative Commons Attribution - NonCommercial - NoDerivatives 4.0 International License

**Cellulose nanocrystals modification by grafting from ring opening
polymerization of a cyclic carbonate**

Michael Lalanne-Tisné^{1,2}, Samuel Eyley¹, Julien De Winter³, Audrey Favrelle-Huret², Wim Thielemans^{1*},
Philippe Zinck^{2*}

¹ Sustainable Materials Lab, Department of Chemical Engineering, KU Leuven, campus Kulak Kortrijk,
Etienne Sabbelaan 53, box 7659, B-8500 Kortrijk, Belgium

*wim.thielemans@kuleuven.be

² Université de Lille, CNRS, Centrale Lille, Univ. Artois, UMR 8181 - UCCS - Unité de Catalyse et Chimie
du Solide, F-59000 Lille, France

*philippe.zinck@univ-lille.fr

³Organic Synthesis and Mass Spectrometry Laboratory (S²MOs), University of Mons - UMONS, 23 Place
du Parc, 7000 Mons, Belgium

27 Abstract

28 Surface modification of cellulose nanocrystals (CNC) by organocatalysed grafting through ring-opening
29 polymerization (ROP) of trimethylene carbonate was investigated. Organocatalysts including an amidine
30 (DBU), a guanidine (TBD), an amino-pyridine (DMAP) and a phosphazene (BEMP) were successfully
31 assessed for this purpose, with performances in the order TBD > BEMP > DMAP, DBU. The grafting ratio
32 can be tuned by varying the experimental parameters, with the highest grafting of 74% by weight obtained
33 in smooth conditions, *i.e* at room temperature in tetrahydrofuran with a low amount of catalyst. This value
34 is much higher than that of typical ring opening polymerizations of cyclic esters initiated from the surface
35 of cellulose nanoparticles. Additionally, DSC analysis of the modified material revealed the presence of a
36 glass transition temperature, indicative of a sufficient graft length to display polymeric behaviour. This is,
37 to our knowledge, the first example of cellulose nanocrystals grafted with polycarbonate arms.

38

39 Keywords:

40 Cellulose nanocrystals, Organocatalysis, Polycarbonate, Nanocellulose, Ring-opening polymerization

41 Chemical compounds studied in this article:

42 Trimethylene Carbonate (PubChem CID: 123834); 1,5,7-Triazabicyclo[4.4.0]dec-5-ene (PubChem CID:
43 79873); 4-Dimethylaminopyridine (PubChem CID: 14284); BEMP phosphazene (PubChem CID:
44 3513851); 1,8-Diazabicyclo(5.4.0)undec-7-ene (PubChem CID: 81184)

45

46 1. Introduction:

47 Polysaccharides, and in particular cellulose, have experienced a rejuvenation of interest in recent years after
48 being slowly replaced by petroleum alternatives during the 20th century in many applications. With the
49 increasing concern over sustainability of many aspects of chemistry and materials science, the surge of
50 interest in these materials is unsurprising as they constitute the bigger fraction of biomass (Habibi, Lucia,
51 & Rojas, 2010). Cellulose nanoparticles in particular have received a lot of attention due to native cellulose
52 availability and their interesting properties such as a high aspect ratio, high young modulus, and low density
53 (Dufresne, 2013). Both cellulose nanofibrils (CNF) and cellulose nanocrystals (CNC) have been widely
54 studied as fillers for composite materials since the work of Favier *et al.* in 1995 who reported on the first

composites reinforced with cellulose nanocrystals. Incorporation of nanocellulose into a polymer matrix has since been studied extensively and has the potential, especially when combined with biodegradable polymers, to produce strong yet fully biodegradable materials. To this end, carbonates are of particular interest, as aliphatic polycarbonates are highly valuable polymers with a very large scope of applications, most notably in textiles, biomedical applications, microelectronics, and packaging (Yu, 2021). As an additional benefit to being biodegradable (Artham & Doble, 2008), aliphatic polycarbonates have also been obtained from renewable sources making them valuable as a potential alternative to petroleum-based polymers (Helou *et al.*, 2010). To produce high performance composite materials, using nanocellulose directly as an additive to polymers has proven to give less than ideal results due to the highly hydrophilic nature of cellulose and its tendency to aggregate. These issues typically lead to a lower than expected mechanical strength and ductility as these are highly dependent on the dispersion of the reinforcing fibre in the polymer matrix and on the strength of the interface (Habibi, 2014).

To find solutions, a large amount of work has been carried out on the surface modification of cellulose nanocrystals, typically using the hydroxyl groups (Eyley & Thielemans, 2014) *via* acetylation (Xu, Wu. Z., Wu. Q., Kuang, 2020), carbamation (Girouard *et al.*, 2016), esterification (Trinh & Mekonnen, 2018), etherification (Sahlin *et al.*, 2018), silanization (Anžlovar, Krajnc, & Žagar, 2020), amidation (Lasseuguette, 2008), and polymer grafting by different methods. While “grafting to” polymerization, *i.e* the process of grafting a pre-synthesized polymer chain to the surface of cellulose can be successful (Azzam *et al.*, 2016), the “grafting from” method is usually the preferred pathway to cellulose modification with polymers as it is better controlled and avoids problems such as steric hindrance (Wohlhauser *et al.*, 2018). The “grafting from” approach has been used to couple many types of polymers on cellulose such as *e.g* polylactones (Habibi *et al.*, 2008; Labet & Thielemans, 2012) and polylactide (Lalanne-Tisné, Mees, Eyley, Zinck, & Thielemans, 2020). In the case of polymer grafting, the main goal is usually to increase the compatibility between the cellulose fibres and a polymer matrix (Thielemans, Belgacem, & Dufresne 2006). Lactones and lactides have received a lot of attention due to their potential in biomedical application (Albertsson & Varma, 2003) as they can undergo hydrolysis *in vivo*. However, polyester hydrolysis generates carboxylic acids, which can be a significant drawback (Lendlein & Langer 2002). Polycarbonates demonstrate much of the same advantages as polyesters when it comes to their degradation *in vivo* (Engler *et al.*, 2013) but they do not generate acidic products during hydrolysis (Kluin *et al.*, 2009). Despite their potential use, however, polycarbonate grafting has not seen much attention, with only some work on grafting on cellulose filter paper (Pendergraph, Klein, Johansson, & Carlmark 2014), synthesis of isosorbide-based polycarbonates (PC) in the presence of cellulose nanocrystals (Park *et al.*, 2019), and grafting of poly(trimethylene carbonate) from starch (Samuel *et al.*, 2014). To our knowledge, the grafting of aliphatic polycarbonates from the surface of cellulose nanocrystals has never been reported before.

To exert control over final properties, it is important to have a well-controlled polymerization reaction. Therefore, the choice of a catalytic system with a high activity and a high level of control is a primary concern. In the case of aliphatic polycarbonates, ring-opening polymerization (ROP) is currently the leading approach as it leads to a living polymerization, therefore satisfying the criteria listed before, *i.e* high activity and high level of control (Jerome & Lecomte, 2008; Penczek, Cypryk, Duda, Kubisa, & Slomkowski, 2007). State of the art ROP allows for the use of many catalysts, including non-toxic metal centres like zinc. However the presence of catalyst traces in the material produced is unwanted for many applications, and metal catalysts are known for being hard to remove completely from polymeric materials (Hafrén & Córdova, 2005). “Immortal” ring-opening polymerization is an approach that has been used for carbonate polymerization and which allows for the use of a small amount of catalyst along with a co-initiator in the form of a protic source. This co-initiator determines the number of chains growing, which gives control over the chain length no matter the quantity of catalyst used while keeping a high catalytic activity (Helou, Miserque, Brusson, Carpentier, & Guillaume, 2008). This approach can also be carried out metal free, as many advances in organocatalysis have led to the emergence of a wide variety of ROP catalysts (Ottou, Sardon, Mecerreyes, Vignolle, & Taton, 2016). While not all these systems are as efficient as metallic catalysts, some are very promising and have shown a high degree of control. In the case of aliphatic carbonates, and in particular trimethylene carbonate (TMC, see Figure 1), base catalysts have been reported to produce polycarbonates with low dispersity (Kamber *et al.*, 2007). Catalysts of interest include amines (dimethylethanolamine, 4-dimethylaminopyridine-DMAP), guanidines (1,5,7-triazabicyclo[4.4.0]dec-5-ene-TBD), amidines (1,8-diazabicyclo[5.4.0]undec-7-ene-DBU), and phosphazenes (2-*tert*-butylimino-2-diethylamino-1,3-dimethylperhydro-1,3,2-diazaphosphorine-BEMP) among others (Helou *et al.*, 2010; Lohmeijer *et al.*, 2006). While ring-opening polymerization of trimethylene carbonate with organic catalysts has been studied extensively in the last decade, small protic molecules such as benzyl alcohol were mostly used as the co-initiator (Helou *et al.*, 2010). Therefore, using cellulose nanocrystals as the protic source to obtain a brush copolymer with polycarbonate is an interesting perspective. Understanding of the reaction and the influence of different parameters would be valuable to increase the general efficiency of polymer grafting on cellulose, a process with a generally low yield (Lalanne-Tisné *et al.*, 2020). In particular, to our knowledge, trimethylene carbonate has never been grafted on the surface of cellulose nanocrystals before. Hence, we report the first synthesis of poly(trimethylene carbonate) grafted cellulose nanocrystals *via* ring opening polymerization and investigate the influence of experimental parameters in an effort to increase the grafting efficiency.

2. Materials and Methods

2.1. Materials

Sulfuric acid (97%) was obtained from VWR and calcium hydride was purchased from Acros Organics. Dichloromethane and ethanol (analytical reagent grade) were obtained from Carlo Erba and cotton wool was obtained from Fischer Scientific. Benzoic acid (99%) and tetrahydrofuran were obtained from Sigma Aldrich and purified through alumina column (Mbraun SPS). 2-*tert*-Butylimino-2-diethylamino-1,3-dimethylperhydro-1,3,2-diazaphosphorine (BEMP, 98%) was also obtained from Acros Organics. 1,8-Diazabicyclo[5.4.0]undec-7-ene (DBU, 99%) was bought from Alpha Aesar and 1,5,7-Triazabicyclo[4.4.0]dec-5-ene (TBD, >98%) from TCI. BEMP, DBU and TBD were introduced, opened and stored in a glovebox and used as received.

Trimethylene carbonate (TMC, 99.5%) was purchased from Actua Chemicals and purified by drying over calcium hydride, filtered under inert atmosphere and then recrystallised. The purified monomer was subsequently stored in a glovebox. 4-Dimethylaminopyridine (DMAP, 99%) was purchased from Aldrich and co-evaporated three times with toluene followed by sublimation under vacuum at 85°C and stored in a glovebox before use.

All chemicals were used as received unless stated otherwise.

Preparation of CNCs

Cotton nanocrystals were prepared by acid hydrolysis of cotton wool for 35 min at 45°C in a 64 wt% aqueous H₂SO₄ solution while stirring constantly (Revol *et al.*, 1992). Deionised water was used to wash the resulting suspension by three successive centrifugations at 10 000 rpm and 10°C for 40 min, replacing the supernatant with deionised water each time. Dialysis under continuous tap water flow was then used to remove residual free acids. After 48 h, the pH of the eluent was checked to be neutral and a homogeneous dispersion of cotton nanocrystals in water was obtained using a Branson sonicator at 10% amplitude for 2 min. The dispersion was subsequently filtered over a fritted glass filter no. 2, and stirred overnight with Amberlite MB-6113 resin to remove non-H₃O⁺ cations. The dispersion was sonicated one last time, frozen in liquid nitrogen, and freeze-dried using a Heto PowerDry PL6000 apparatus from Thermo Scientific under a vacuum of 2 bars. In addition to this procedure commonly followed in the literature to prepare cellulose nanocrystals, a further purification was performed to remove surface adsorbed impurities that adsorb onto the nanocrystal surface (Labet & Thielemans, 2011). After freeze-drying, the cotton nanocrystals were Soxhlet extracted for 24h using ethanol as a solvent. The nanocrystals were subsequently dried in a vacuum oven (0.5 bar) at 50°C and then dried further under ultra-high vacuum (Pfeiffer DCU 100) at 10⁻⁶ bars for 4

days. The container used for the drying process was then tightly closed, filled with argon, and placed in a glovebox.

2.2. Ring-opening polymerization of TMC on CNC surface

All experiments were carried out under inert atmosphere in a glovebox unless stated otherwise.

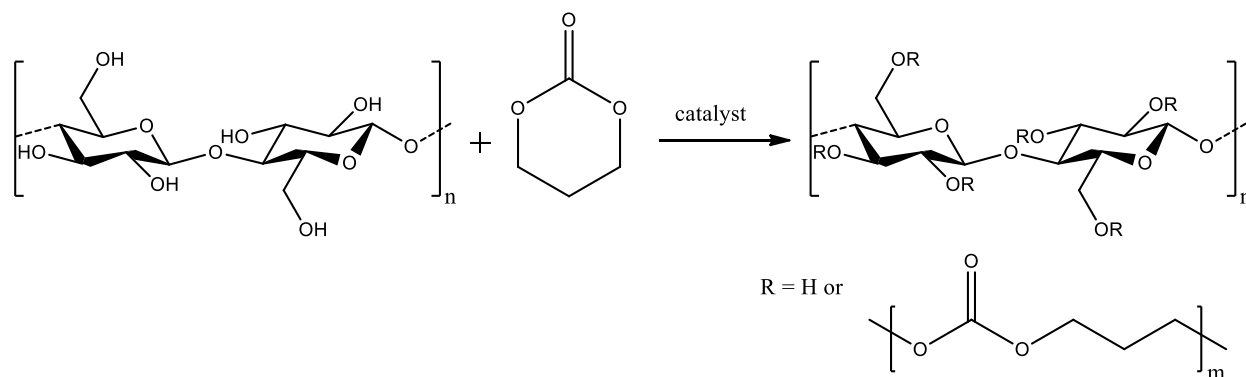


Figure 1: General reaction scheme of the ring-opening polymerization of trimethylene carbonate co-initiated by hydroxyls present on the surface of cellulose nanocrystals

In a typical reaction, a stir bar was placed in a small reactor, along with a specified amount of CNCs. The molar ratio used are specified in Table 1 and Table 2 and based of the molecular weight of one glucose ring bearing one primary OH. THF was added and the mixture was stirred for 30 minutes to disperse the CNCs. Trimethylene carbonate was then added and left to stir until complete dissolution. Subsequently, the catalyst was added while stirring and the reactor was placed in an oil bath set at a given temperature. After the desired duration, the reaction was quenched using benzoic acid and dichloromethane addition, and the mixture was filtered through a Soxhlet extraction thimble. A sample of the crude mixture was taken for NMR analysis, and the modified CNCs were purified by Soxhlet extraction twice, first with dichloromethane (24 hours), and then with ethanol (24 hours).

The modified nanocrystals were then dried under vacuum on a Schlenk line (< 1 mbar) for 24 hours.

The homopolymer produced as a side reaction was recovered from the first Soxhlet extraction mixture after evaporation of the dichloromethane.

Characterization methods, apparatus, calculation method to determine grafting, conversion and yield, and additional information about experimental procedures are all available in Supporting Information Appendix A.

3. Results and discussion

3.1. Catalyst screening

Table 1: Ring-opening polymerization of TMC initiated from the surface of CNC in the presence of various organocatalysts at 25°C in THF

Entry	Catalyst	TMC / Catalyst / OH ^[a]	Time (h)	Polycarbonate grafting ^[b] (wt%)	Conversion ^[c] (%)	Grafting Yield ^[d] (%)	M _n homopolymer ^[e] (g.mol ⁻¹)	Đ _M ^[f]
1	Blank	500/0/50	5	2	4	0.3	NA	NA
2	TBD	500/1/50	5	51	99	16.5	19700	1.8
3	BEMP	500/1/50	3	24	45	5.0	35400	1.9
4	BEMP	500/1/50	5	35	52	8.6	33500	1.8
5	BEMP	500/1/50	16	37	52	9.3	33500	1.8
6	DMAP	500/0.5/50	5	13	6	2.4	NA	NA
7	DMAP	500/2/50	5	3	7	0.5	NA	NA
8	DMAP	500/5/50	5	12	6	2.2	2100	1.2
9	DBU	500/1/50	3	18	9	3.5	NA	NA
10	DBU	500/1/50	5	12	8	2.2	NA	NA

[a] Calculated using moles of glucose rings (162.14 g/mol), and considering 1 primary OH per ring [b] Determined by elemental analysis (calculation based on hydrogen content (%H) and carbon content (%C)) and corrected for adsorbed water using TGA. [c] Calculated *via* ¹H NMR to determine monomer/polymer ratio and corrected to include monomer grafted [d] Ratio of initial monomer to monomer grafted. [e] Determined by SEC of homopolymer vs. polystyrene standards and corrected with a correction factor of 0.57, 0.73 or 0.88 based on size measured (Palard *et al.* 2007). [f] Molar mass distribution calculated from SEC of homopolymer.

The performances of the different organic catalysts, namely TBD, BEMP, DMAP and DBU (shown in Figure 2) to polymerize TMC from the surface of cellulose nanocrystals were evaluated in THF at room temperature. The different catalysts were selected from their ability to catalyse ROP of TMC in the presence of an alcohol (Helou *et al.*, 2010). The TMC/catalyst/OH ratio was mostly kept at 500/1/50. Table 1 displays the most significant results.

In the absence of catalyst, significant conversion of the monomer into either grafts or homopolymer was not achieved (Table 1, entry 1), showing the clear need to use a catalyst.

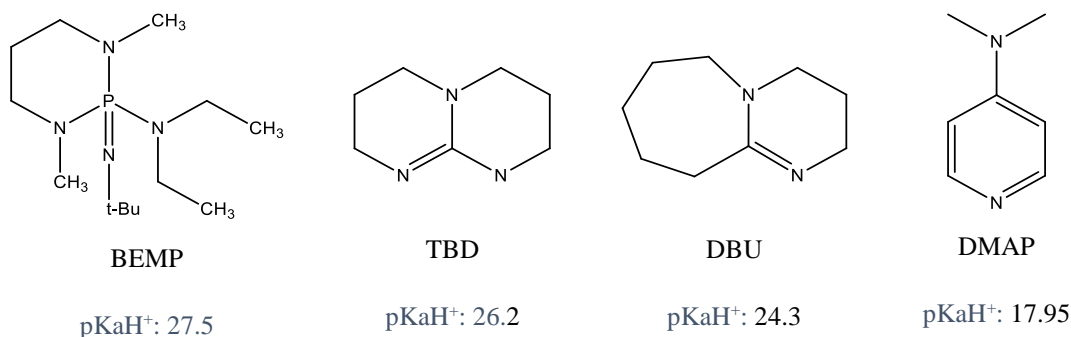


Figure 2: Structure of the organocatalysts used in this study. pKa values in acetonitrile (Ishikawa, 2009; Kaljurand *et al.*, 2005)

At a typical ratio of 500/1/50 (TMC/catalyst/OH), TBD was shown to reach full conversion of the monomer within 5 hours, and resulted in modified CNCs containing of 51% grafted polymer (Table 1, entry 2), a fairly high value for typical “grafting from” of polymer through ring opening polymerization from the surface of nanocellulose. Similarly, a significant amount of monomer was converted to homopolymer (yield of 16% for grafting), which shows an important competition between grafting of the monomer and homopolymerization. However, it is common for grafting on cellulose to use a large excess of monomer to increase the amount of grafting at the cost of efficiency (Lalanne-Tisné, *et al.*, 2020; Miao & Hamad, 2016). Molar mass dispersity of the homopolymer was found at an acceptable value of 1.8 that is significantly higher than usual values obtained for typical homopolymerizations (Nederberg *et al.*, 2007). The broader distribution can be explained because it is a side reaction involving water and ethanol as co-initiators that are still entrapped in the CNCs after purification. In addition, water and ethanol can also be involved in hydrolysis and transcarbonatation reactions respectively. This can be seen from the MALDI ToF mass spectra of the precipitated polymer showing the corresponding chain ends (details in Supporting Information Appendix A).

Using similar reaction conditions for BEMP (entries 3-5), a phosphazene catalyst, showed quite different results. Full conversion was not reached, and after increasing the reaction time from 3 to 5 hours, BEMP conversion only reached 52%. Further increasing the reaction time to 16 hours did not increase monomer conversion. Despite the lower conversion values, grafting on cellulose was achieved with this catalyst, and up to 37% grafts were achieved in the modified CNCs, showing that this catalyst, while less efficient than TBD using similar parameters, leads to substantial grafting.

The reactions conducted with DMAP (entries 6-8) and DBU (entries 9-10) did not perform as well as the others under the same reaction conditions (room temperature, 5h), with NMR analysis showing very low conversion. The resulting grafting was rather low for both catalyst (18% maximum) under these conditions, and no oligomers could be recovered by precipitation to allow for SEC analysis. This is believed to be due to their likely low average molecular weight.

We can try to explain the superior performance of TBD. TBD, unlike the other catalysts tested, possesses a secondary amine group, giving it great potential for catalysis *via* hydrogen bonding. It is also interesting to note that unlike DBU, which can operate by a basic and a nucleophilic mechanism, TBD can catalyse transesterification reactions by dual activation *via* H-bonding (Simón & Goodman, 2007; Stanley *et al.*, 2019). Having a catalyst that can use both mechanisms may result in a better reaction due to the ability of the catalyst to go in between intermolecular bonding (similarly to how a protic solvent gives a better dispersion of CNCs). In addition, DBU and DMAP may favour homopolymerization due to their ability to

perform a nucleophilic attack on the monomer, which is not the case for the BEMP phosphazene, that leads to an intermediary grafting ratio.

When looking at results for homopolymerization of trimethylene carbonate (Helou *et al.* 2010), it is worth noting that TBD is also the most active catalyst in bulk, and full conversion is achieved much faster at lower temperatures when compared to DMAP and DBU. As the work presented here is carried out in solvent but at room temperature, it is possible that the activity of some of the catalysts (except for TBD) is reduced as the activation requires more energy. However, further testing at higher temperature with all the catalyst was not explored as we observed browning of the CNC at temperatures as low as 40°C in the presence of THF and TBD (see next section).

Comparing the pK_a of all 4 bases, TBD in acetonitrile does not come up as the strongest base (25.96), with BEMP having a higher pK_a (27.5), despite its superiority when it comes to grafting TMC on cellulose. TBD is however a stronger base than DMAP and DBU, which could explain partially the better results obtained when comparing these 3 bases. As for BEMP, it is a much bulkier catalyst, therefore steric hindrance may be the cause for the lower activity when compared to TMC, in particular for the grafting onto CNC. This can be exemplified as despite the subpar grafting efficiency on CNCs with BEMP, the extracted homopolymer showed a higher M_n than the homopolymer recovered after full conversion with TBD.

As the screening of catalysts showed a more efficient grafting with TBD, this reaction was studied further, in order to assess the influence of the reaction conditions.

3.2. Influence of experimental parameters for the TBD catalysed grafting

As the polymerization of TMC has also been performed in bulk (Helou *et al.*, 2010), the grafting reaction on the surface on CNCs was also carried in bulk as comparison (entry 11, Table 2). Despite homopolymerization of TMC being very quick under bulk conditions, the reaction with cellulose did not go to full conversion within an hour. However, the polycarbonate content of modified CNCs did reach 47%, a value comparable to the content obtained by grafting in THF. The viscosity is a major issue in bulk reactions as the melted monomer is not a good medium to disperse CNCs, resulting in poor homogeneity of the final material and a greater difficulty to redisperse the modified cellulose in solvent, rendering its use more complicated. The high viscosity is also likely a cause for the lower conversion, as the reaction slows down considerably with homopolymer production. Lastly, the bulk reaction, as expected, shows a much higher dispersity for the synthesized homopolymer, indicating some loss of control over the polymerization reaction.

THF was used as the main solvent as it had shown to dissolve well TBD, TMC, poly(trimethylene carbonate), and to be a good solvent for CNC dispersion. Some other common solvents were assessed, but worse results were obtained (additional information in SI).

Table 2: Ring-opening polymerization of TMC initiated from the surface of CNC in the presence of TBD in THF for 5 hours

Entry	TMC / Catalyst / OH ^[a]	T (°C)	Polycarbonate grafting ^[b] (wt%)	Conversion ^[c] (%)	Grafting Yield ^[d] (%)	M _n homopolymer ^[e] (g.mol ⁻¹)	D _M ^[f]
2	500/1/50	25	51	99	16.5	19700	1.8
11 ^[g]	500/1/50	65	47	33	14.1	11200	3.0
12 ^[h]	500/1/50	25	60	99	23.8	19600	1.9
13	500/1/50	0	54	99	18.7	16500	2.0
14	500/1/50	40	51	99	16.5	14100	2.3
15	500/1/50	60	52	99	17.2	9700	1.8
16 ^[i]	500/1/50	25	7	99	1.2	NA	NA
17	500/1/40	25	49	99	12.2	18700	1.7
18	500/1/30	25	49	99	9.2	23100	1.7
19 ^[j]	500/1/50	25	53	99	17.9	12100	2.0
20	500/2/50	25	9	99	1.6	26700	1.8
21	500/5/50	25	9	99	1.6	2200	1.3
22	500/0.5/50	25	74	99	45.2	7100	1.8
23	500/0.25/50	25	64	78	28.2	11400	1.6
24	250/0.5/50	25	57	99	42.1	11100	1.7
25	125/0.5/50	25	47	99	56.3	4600	1.8
26	62.5/0.5/50	25	23	99	37.9	NA	NA
27	250/1/50	25	50	99	31.8	13700	1.9
28	125/1/50	25	41	99	44.1	12900	1.8

[a] Calculated using moles of glucose rings (162.14 g/mol), and considering 1 primary OH per ring [b] Determined by elemental analysis (calculation based on hydrogen content (%H) and carbon content (%C)) and corrected for adsorbed water using TGA. [c] Calculated *via* ¹H NMR to determine monomer/polymer ratio and corrected to include monomer grafted [d] Ratio of initial monomer to monomer grafted. [e] Determined by SEC of homopolymer vs. polystyrene standards and corrected with a correction factor of 0.57, 0.73, or 0.88 based on size measured (Palard *et al.* 2007). [f] Molar mass distribution calculated from SEC of homopolymer. [g] Bulk reaction. [h] Reaction done over 24 hours instead of 5. [i] Reaction performed outside the glovebox. [j] Stirred for 24h and sonicated prior to reaction to maximize dispersion of CNC. NA: not available as oligomers, i.e too short to precipitate in cold methanol

As shown previously (entry 11), the polymerization of TMC was total after 5 hours, however a reaction in similar conditions was also performed over 24 hours (entry 12) to evaluate the activity of TBD over longer period of time, as it has been reported to be capable of depolymerization (Meimoun *et al.*, 2020). In the case of poly(trimethylene carbonate) grafted CNCs, a small increase in grafting content can be measured after 24 hours of reaction, however the average molecular weight of the produced homopolymer started decreasing, showing potential signs of depolymerization or transcarbonation reactions. Therefore 5 hours was the favoured reaction time for most reaction, as it allowed for a good control over grafting while having good conversion, and a very good reproducibility (repeated reactions available in SI).

At the typical ratio of TMC/Cat/OH of 500/1/50, variation in temperature was tested to determine its influence on the grafting reaction. At first glance, the temperature did not appear to change the amount of grafting by a significant amount, as increasing the temperature to 40°C (entry 14) or 60°C (entry 15) yielded CNCs with 51% and 52% grafts respectively (compared to entry 2). However, at temperatures as low as 40°C, browning of the CNCs was observed and became more pronounced at higher temperature, indicating a potential degradation of the material. A shortening of the homopolymer chains is further observed as the reaction temperature increases, indicating of possible depolymerization / chain scission reactions in the presence of TBD, which has been reported for both polycarbonates (Li, Sablong, van Benthem, & Koning, 2017) and polylactides (Meimoun *et al.*, 2020). A reaction at 0°C was also performed using an ice bath to determine if a lower temperature could favour grafting over homopolymerization (entry 13), however the results obtained for the grafting of CNC were in the same range (>50%) as the reaction performed at room temperature (RT). The temperature used for the rest of the reaction was therefore set to RT (controlled by an oil bath) to avoid any degradation of the material and to keep the reaction more energy efficient.

A reaction was then performed under inert atmosphere, but not under glovebox conditions, to evaluate how sensitive the efficiency of the grafting was regarding the presence of water and other impurities (entry 16). Prior to the reaction, CNCs and TMC were dried using a vacuum and an argon line rather than ultra-high vacuum. THF was used after purification over alumina, similarly to experiments performed inside the glovebox. Multiple argon/vacuum cycles were used to ensure inert atmosphere was achieved. Under these conditions, a low amount of grafting (7 vs. 51% in entry 2) as well as the short chain length of the homopolymer (impossible to precipitate in cold methanol) showed the prevalence of initiation by traces of water and ethanol. Due to CNCs being hydrophilic, it is hard to remove significant traces of water from them without extreme conditions (10^{-6} bar of vacuum), as well as ethanol from the purification steps of preparing CNCs. This reaction shows that in order to maximize grafting efficiency purification of the different chemicals a thorough drying of the cellulose is required, and working in a glovebox is useful.

In an attempt to increase grafting on cellulose, reactions were then performed with an increased ratio of TMC/CNC by decreasing the quantity of cellulose used. Surprisingly, increasing the quantity of monomer did not lead to a significant improvement in the grafting amount on cellulose (entries 17-18), which seems to reach a maximum at around 50%, a result similar to other reactions (entry 2). This shows that simply increasing the quantity of monomer used in the reaction is an ineffective way to increase the maximum amount of grafting on the surface of CNC.

To determine if the availability of the hydroxyl groups on the surface of cellulose is an important factor, a reaction was performed on a batch of CNC in THF with increased effort at individualization of CNCs. The mixture of cellulose and solvent was prepared in the glovebox, then closed tightly and stirred over 24 hours

vs. 30 min previously used. A sonication bath was also used in burst of 5 minutes over the 24 hours. The results obtained (entry 19) when compared to a “typical” reaction showed that increased effort for maximum individualization of CNCs did not have a significant impact as the grafting obtained was also around the 50% mark.

The influence of catalyst loading was further assessed. Using a typical ratio TMC/TBD/OH of 500/1/50 showed good results and a grafting of around 50%. Increasing the catalyst ratio to 2 equivalents *vs.* OH (entry 20) however lowered the grafting % on CNCs by a significant amount, whereas the length of the homopolymer increased, indicating that increasing the TBD amount favours homopolymerization. Increasing the amount of catalyst further to 5 equivalents (entry 21) yielded a similar amount of grafting onto the CNCs than entry 20 (9%), but the average molecular weight of the isolated polymer was significantly smaller ($< 3000 \text{ g.mol}^{-1}$). As mentioned previously, TBD is not only capable of polymerization, but also depolymerization under the right circumstances *via* a nucleophilic attack on the carbonyl moieties (Meimoun *et al.* 2020). In the case of polylactide, the use of 5 equivalents of TBD decreased the average molecular of the resulting polymer more than tenfold, a result very similar to what is observed in this work for the polycarbonate.

As opposed to increasing the catalyst quantity, lowering the amount of TBD used for the reaction to 0.5 equivalents showed an improvement in the grafting on CNCs with a material composed of up to 74% polycarbonate grafts by weight and a grafting yield of 46% (entry 22). M_n of the homopolymer obtained was lower, which can simply be explained by the increased quantity of monomer turned into grafts rather than homopolymer.

Decreasing the quantity of catalyst further resulted in a decrease in the amount of grafting to 64% (entry 23), which is an improvement over the result obtained with 1 equivalent (entry 2) but a setback compared to reactions performed with 0.5 equivalent (entry 22). Moreover, the low concentration of TBD led to a slower reaction, and obtaining full conversion became more difficult.

To improve the grafting efficiency with respect to the total amount of monomer used, reactions with 0.5 equivalent of TBD (shown to have the best results) and successively lower amounts of monomer were carried out.

The grafting % decreased from 74% to 57% (entry 22 *vs.* 24) when the monomer concentration was halved, but the grafting yield stayed within the same range at 42%. While this is not an improvement, it however, allows one to obtain CNCs with around 50% grafts with significantly less monomer loss than some previous experiments (*e.g* entry 2). Lowering the amount of monomer further continued to reduce the % grafting

(47%) but led to an increased yield of 56% which is a good value for grafting of a polymer on cellulose, as this parameter is usually overlooked in favour of trying to reach a maximum amount of grafting.

A similar reaction was also performed with a typical 1 equivalent TBD to compare to the grafting yield obtained with 0.5 equivalents. As previously shown, the grafting % obtained is superior using a lower quantity of catalyst, leading to a higher grafting yield.

Overall, this shows that a wide range of grafting % is possible, and specific values can be targeted using the right amount of catalyst (typically 0.5 eq) without having to use a large excess of monomer, while keeping the grafting yield as high as possible.

3.3. Characterization of the poly(trimethylene carbonate)-grafted CNC as a function of the grafting ratio

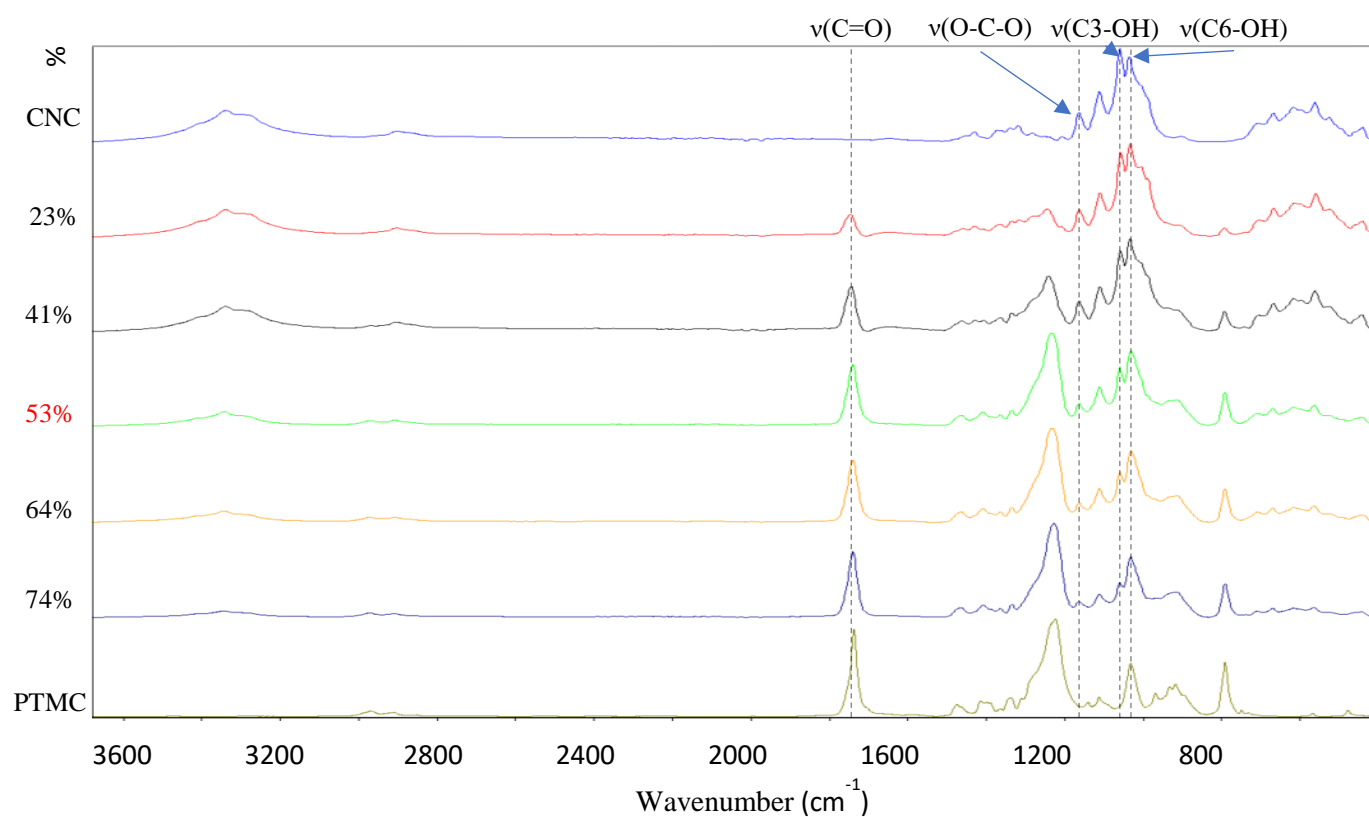


Figure 3: FT-IR spectra of unmodified cellulose nanocrystals (CNC) and grafted one with different graft content after purification by Soxhlet extraction. PTMC of 154000 g/mol extracted from soxhlet and purified by precipitation. Grafted CNCs corresponding to refe

In addition to elemental analysis, FT-IR was used to determine the success of the grafting reaction (Figure 3). As expected, both modified and unmodified cellulose spectra resemble each other. However, 2 bands characteristic to our grafts are visible for modified cellulose. First, the band at 1754 cm⁻¹ can be identified

as a carbonyl stretch $\nu(\text{C}=\text{O})$, thus confirming the successful incorporation of the carbonate moieties onto CNCs. A second characteristic band is observed at 1229 cm^{-1} corresponding to $\nu(\text{C}-\text{O})$ stretching (Nyquist & Potts, 1961). As shown in Figure 3, the relative intensity of both bands increased with the grafting content, thus confirming the results determined by elemental analysis and TGA. Lastly, the ratio of absorption band at 1059 cm^{-1} corresponding to $\nu(\text{C3}-\text{OH})$ to $\text{C}-\text{O}-\text{C}$ stretching at 1160 cm^{-1} (Marechal & Chanzy, 2000), decreases with increasing grafting ratio which shows the successful esterification of the secondary alcohol in the C3 position. The band at 1032 cm^{-1} corresponding to $\nu(\text{C6}-\text{OH})$ increases with increasing grafting ratio, as terminal OH of the polycarbonate chains appear in this region as well. As a consequence, grafting on the C6 position is not “visible” by FTIR, as both primary and secondary C-OH of cellulose are replaced by the primary terminal C-OH of the polymer at 1032 cm^{-1} . Note that $\nu(\text{C2}-\text{OH})$ cannot be discussed here as the polymer has a band in the area.

X-ray photoelectron spectroscopy can give additional insight into the composition of the modified CNCs at

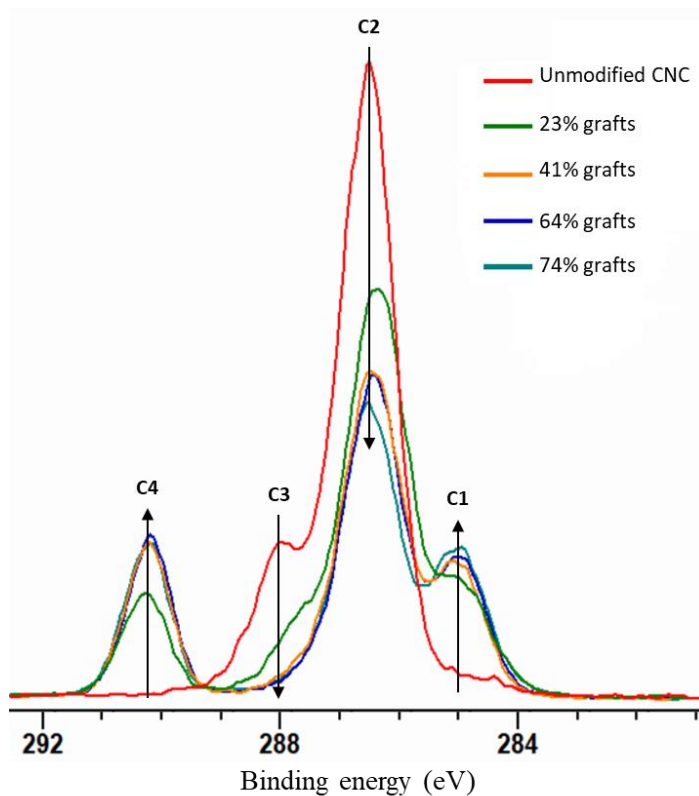


Figure 4: Carbon 1s X-ray photoelectron spectroscopy (XPS) scan of cellulose nanocrystals grafted with different poly(trimethylene carbonate content). Grafted CNCs corresponding to reference in Table 2: entry 26 (23%) entry 28 (41%), entry 23 (64%), entry 22 (74%)

a surface level. In the C1s high resolution scan (Figure 4), the aliphatic C-C carbon contribution (C1) at 285 eV is shown to increase rapidly with grafting, as cellulose units do not contain aliphatic carbons, unlike trimethylene carbonate. With an increasing amount of graft content, the relative intensity of the C1

contribution increases and then appears to reach a maximum, at the contribution amount expected for pure poly(trimethylene carbonate) chains indicating that no cellulose contribution is visible anymore. As opposed to C1, the C2 and C3 contributions to the C1s signal, corresponding to C-O and O-C-O environments respectively, both decreased with an increasing amount of grafts, as poly(trimethylene carbonate) contributes less to the C-O signal than cellulose, and does not contribute to the O-C-O signal. Finally, the O-C=O contribution (C4) increased with grafting content, similarly to C1 as the carbonate function is the only contribution to this peak. The results obtained from elemental analysis, along with form of characterization are therefore confirmed with the XPS data.

With poly(trimethylene carbonate) being a highly hydrophobic material, grafting CNCs with it will change its interaction with water significantly. To quantify this, grafted CNCs were used in contact angle

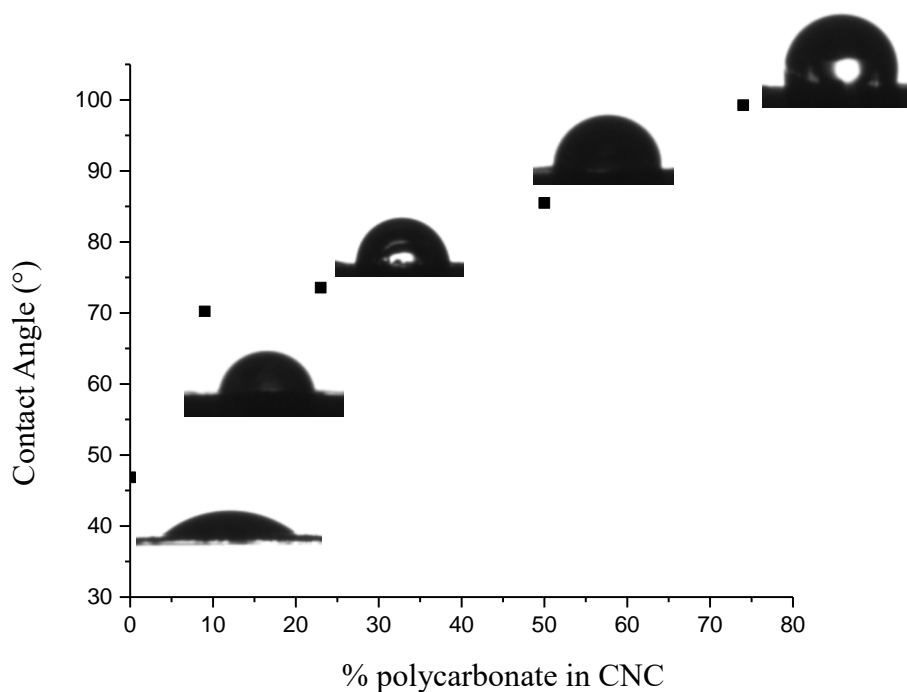


Figure 5: Contact angle of a water droplet on the surface of CNC modified with different polycarbonate content. Grafted CNCs corresponding to reference in Table 2: entry 9 (9%) entry 26 (23%), entry 2 (51%), and entry 22 (74%)

measurements with water. The water contact angle increased rapidly with the poly(trimethylene carbonate) content of the cellulose sample (Figure 5), in line with the length of the graft in the brush copolymer structure. For a poly(trimethylene carbonate) content as low as 9%, the increase in hydrophobicity is significant, which then increases more slowly as the carbonate content increased, up to a value close to that of pure PTMC reported in the range 90-110°C (Brossier et al., 2021; Yao et al., 2017). This might be related to an increasing coverage of the CNC by PTMC, ranging from partial to almost full. It is noteworthy that the contact angle and thus the wettability can be controlled by targeting the proper polycarbonate grafting

ratio. As a result, we believe that this increase in hydrophobicity shows good signs for the potential incorporation of these nanoparticles in a polymer matrix for composite applications.

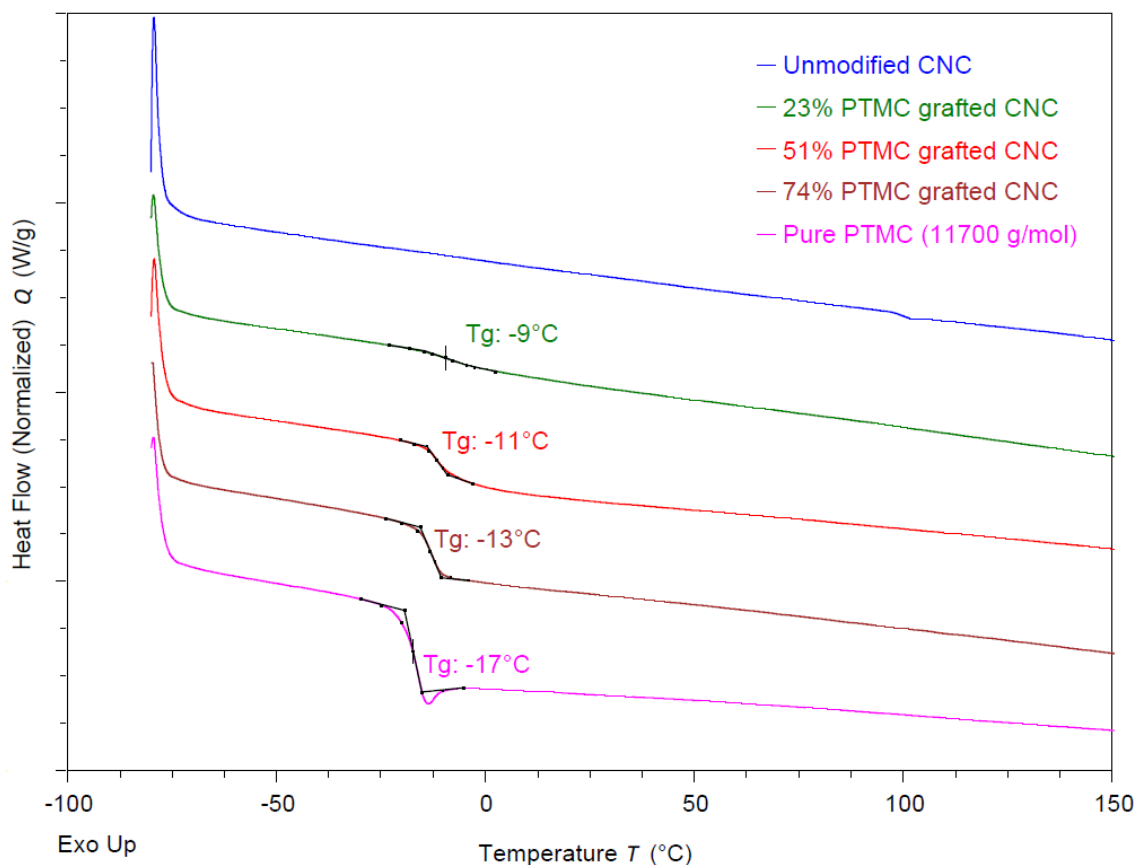


Figure 6: Differential Scanning Calorimetry graphs of CNC, poly(trimethylene carbonate) (PTMC) and modified CNC during the second heating at 10°C/min. . Grafted CNCs corresponding to reference in Table 2: entry 26 (23%), entry 2 (51%), and entry 22 (74%)

DSC analyses were conducted to obtain more information on the thermal behaviour of the grafts. The samples were heated from -80 to 190°C, as the glass transition temperature (T_g) of poly(trimethylene carbonate) is below 0 °C. For unmodified CNCs, no T_g or melting point were observed, as expected (Figure 6). For grafted CNCs, a glass transition was observed for all samples in the same range as the T_g of pure poly(trimethylene carbonate), but with slightly higher values. With a graft content as low as 23%, a T_g at -9°C can be recorded, indicative of the presence of poly(trimethylene carbonate) grafts. As the carbonate content increased, the T_g decreased and progressively moved towards the value for poly(trimethylene carbonate) homopolymer (11700 g.mol⁻¹) at -17°C, without ever reaching it. This phenomenon could be attributed to a lower mobility of the chain closer to the CNC backbone, their relative amount decreasing with higher grafting values. Overall, this shows that polymer grafts on cellulose nanocrystals are of sufficient length to showcase polymeric behaviour. In addition, we also measured the T_g of non-grafted homopolymers of similar molecular weight and compared it with that of the grafted polymer (see SI section

S12). The 3 homopolymers of *ca.* 20 000 g/mol show a T_g of *ca.* -16/-17 °C, whereas the T_g of the grafted CNC are in the range -10 to -13°C, which tend to confirm the occurrence of a true grafting.

In order to know whether the cellulose nanocrystals retain their structure following grafting, wide-angle X-ray scattering was used to determine the crystallinity of the pristine and PTMC grafted CNC samples. The X-ray scattering data was fitted with the crystal structure of cellulose I β , and the amorphous contribution to the scattering determined. As no melting peak was seen in the DSC data, we know that the PTMC will be included in the amorphous contribution to the scattering data. Therefore, considering the amount of PTMC in the sample, changes in crystallinity of the cellulose ($\Delta\chi_{c, \text{cellulose}}$) can be determined as the difference in crystallinity between the starting material and the product ($\Delta\chi_{c, \text{sample}}$), minus the expected contribution from PTMC (ϕ_{PTMC} – the volume fraction of PTMC) as shown in Table 3.

Table 3: The calculated sample crystallinity based on WAXS measurements for all samples

Sample	$\chi_{c, \text{sample}}$	$\Delta\chi_{c, \text{sample}}$	ϕ_{PTMC}	$\Delta\chi_{c, \text{cellulose}}$
Unmodified CNC	0.99	-	0	0
23% PTMC-g-CNC	0.68	-0.31	0.27	-0.04
41% PTMC-g-CNC	0.56	-0.43	0.46	0.03
51% PTMC-g-CNC	0.37	-0.62	0.56	-0.06
64% PTMC-g-CNC	0.26	-0.73	0.69	-0.04
74% PTMC-g-CNC	0.14	-0.85	0.78	-0.07

The data on the grafted samples shows only around 5% change in cellulose crystallinity when the contribution from amorphous PTMC is removed. This change could be due to peeling of the surface chains of the CNC during grafting, however, given the lack of trend in $\Delta\chi_{c, \text{cellulose}}$, and the wide standard deviation in the values, it is possible that this reflects the error in the calculation of the sample crystallinity by this methodology.

Conclusion

Ring-opening polymerization (ROP) of trimethylene carbonate was performed using cellulose nanocrystals as a co-initiator in the presence of 4 organocatalysts, *i.e.* DMAP, DBU, TBD and BEMP). The overall performances considering conversion, grafting ratio and yield are TBD > BEMP > DBU, DMAP. After optimization, a grafting ratio as high as 74% could be reached using TBD, corresponding to a material composed by weight of almost $\frac{3}{4}$ polycarbonate grafts. The reaction was performed at room temperature with a low concentration of the catalyst, 0.5% vs. TMC and 500 equiv. TMC per glucose unit. This led to a

material with T_g and contact angle close to that of poly(trimethylene carbonate). The use of a single step reaction, under mild conditions while keeping grafting yield high is of great interest to produce CNC with a controlled amount of grafts. Furthermore, we were able to show some of the most influential parameters with respect to grafting content, providing some insight on the chemistry behind cellulose modification. The contact angle can be tuned from *ca.* 50 to 100° by adjusting the grafting ratio. Lastly, DSC results revealed the polymeric behaviour of the grafts, confirming the successful grafting of polycarbonate chains of sufficient length to have high potential as reinforcement fillers in composite materials. To our knowledge, this is the first reported chemical modification of cellulose nanocrystals with trimethylene carbonate, and the first example of a ROP-based grafting from process attaching polycarbonate chains onto CNCs.

4. Acknowledgement

The authors are grateful to Aurélie Malfait for SEC measurements, and Gertrude Kignelman for the help with contact angle analysis. The authors also acknowledge financial support from the Initiatives for Science, Innovation, Territories and Economy (I-SITE) Lille Nord – Europe (MLT PhD fellowship), from Research Foundation Flanders (grant G0C6013N), KU Leuven (grant C14/18/061) and from the European Union's European Fund for Regional Development, Flanders Innovation & Entrepreneurship, and the Province of West-Flanders for financial support in the Accelerate³ project (Interreg Vlaanderen-Nederland program). Université de Lille, Chevreul Institute (FR 2638), Ministère de l'Enseignement Supérieur de la Recherche et de l'Innovation, Région Hauts de France are also acknowledged for supporting and funding partially this work.

5. References:

- Albertsson, A.-C., & Varma, I. K. (2003). Recent Developments in Ring Opening Polymerization of Lactones for Biomedical Applications. *Biomacromolecules*, 4(6), 1466–1486.
- Anžlovar, A., Krajnc, A., & Žagar, E. (2020). Silane modified cellulose nanocrystals and nanocomposites with LLDPE prepared by melt processing. *Cellulose*, 27(10), 5785–5800.
- Artham, T., & Doble, M. (2008). Biodegradation of Aliphatic and Aromatic Polycarbonates: Biodegradation of Aliphatic and Aromatic Polycarbonates. *Macromolecular Bioscience*, 8(1), 14–24.
- Azzam, F., Heux, L., & Jean, B. (2016). Adjustment of the Chiral Nematic Phase Properties of Cellulose Nanocrystals by Polymer Grafting. *Langmuir*, 32(17), 4305–4312.
- Brossier, T., Volpi, G., Vasquez-Villegas, J., Petitjean, N., Guillaume, O., Lapinte, V., & Blanquer, S. (2021). Photoprintable Gelatin- *graft* -Poly(trimethylene carbonate) by Stereolithography for Tissue Engineering Applications. *Biomacromolecules*, 22(9), 3873–3883.
- Dufresne, A. (2013). Nanocellulose: a new ageless bionanomaterial. *Materials Today*, 16(6), 220–227.
- Engler, A. C., Chan, J. M. W., Fukushima, K., Coady, D. J., Yang, Y. Y., & Hedrick, J. L. (2013). Polycarbonate-Based Brush Polymers with Detachable Disulfide-Linked Side Chains. *ACS Macro Letters*, 2(4), 332–336.
- Eyley, S., & Thielemans, W. (2014). Surface modification of cellulose nanocrystals. *Nanoscale*, 6(14), 7764–7779.
- Favier, V., Chanzy, H., & Cavaille, J. Y. (1995). Polymer Nanocomposites Reinforced by Cellulose Whiskers. *Macromolecules*, 28(18), 6365–6367.
- Girouard, N. M., Xu, S., Schueneman, G. T., Shofner, M. L., & Meredith, J. C. (2016). Site-Selective Modification of Cellulose Nanocrystals with Isophorone Diisocyanate and Formation of Polyurethane-CNC Composites. *ACS Applied Materials & Interfaces*, 8(2), 1458–1467.
- Habibi, Y. (2014). Key advances in the chemical modification of nanocelluloses. *Chem. Soc. Rev.*, 43(5), 1519–1542.

454 Habibi, Y., Goffin, A.-L., Schiltz, N., Duquesne, E., Dubois, P., & Dufresne, A. (2008). Bionanocomposites
 455 based on poly(ϵ -caprolactone)-grafted cellulose nanocrystals by ring-opening polymerization. *Journal of*
 456 *Materials Chemistry*, 18(41), 5002.

457 Habibi, Y., Lucia, L. A., & Rojas, O. J. (2010). Cellulose Nanocrystals: Chemistry, Self-Assembly, and
 458 Applications. *Chemical Reviews*, 110(6), 3479–3500.

459 Hafrén, J., & Córdova, A. (2005). Direct Organocatalytic Polymerization from Cellulose Fibers: Direct
 460 Organocatalytic Polymerization from Cellulose Fibers. *Macromolecular Rapid Communications*, 26(2), 82–
 461 86.

462 Helou, M., Miserque, O., Brusson, J.-M., Carpentier, J.-F., & Guillaume, S. M. (2010). Organocatalysts for
 463 the Controlled “Immortal” Ring-Opening Polymerization of Six-Membered-Ring Cyclic Carbonates: A
 464 Metal-Free, Green Process. *Chemistry - A European Journal*, 16(46), 13805–13813.

465 Helou, M., Miserque, O., Brusson, J.-M., Carpentier, J.-F., & Guillaume, S. M. (2008). Ultraproductive,
 466 Zinc-Mediated, Immortal Ring-Opening Polymerization of Trimethylene Carbonate. *Chemistry - A*
 467 *European Journal*, 14(29), 8772–8775.

468 Ishikawa T, editor. Superbases for organic synthesis: guanidines, amidines and phosphazenes and related
 469 organocatalysts. Chichester: John Wiley & Sons, Ltd; 2009; 336 pp

470 Jerome, C., & Lecomte, P. (2008). Recent advances in the synthesis of aliphatic polyesters by ring-opening
 471 polymerization. *Advanced Drug Delivery Reviews*, 60(9), 1056–1076.

472 Kaljurand, I., Kütt, A., Sooväli, L., Rodima, T., Mäemets, V., Leito, I., & Koppel, I. A. (2005). Extension
 473 of the Self-Consistent Spectrophotometric Basicity Scale in Acetonitrile to a Full Span of 28 p K a Units:
 474 Unification of Different Basicity Scales. *The Journal of Organic Chemistry*, 70(3), 1019–1028.

475 Kamber, N. E., Jeong, W., Waymouth, R. M., Pratt, R. C., Lohmeijer, B. G. G., & Hedrick, J. L. (2007).
 476 Organocatalytic Ring-Opening Polymerization. *Chemical Reviews*, 107(12), 5813–5840.

477 Kluin, O. S., van der Mei, H. C., Busscher, H. J., & Neut, D. (2009). A surface-eroding antibiotic delivery
 478 system based on poly-(trimethylene carbonate). *Biomaterials*, 30(27), 4738–4742.

479 Labet, M., & Thielemans, W. (2011). Improving the reproducibility of chemical reactions on the surface
 480 of cellulose nanocrystals: ROP of ϵ -caprolactone as a case study. *Cellulose*, 18(3), 607–617.

481 Labet, M., & Thielemans, W. (2012). Citric acid as a benign alternative to metal catalysts for the production
 482 of cellulose-grafted-polycaprolactone copolymers. *Polymer Chemistry*, 3(3), 679

483 Lalanne-Tisné, M., Mees, M. A., Eyley, S., Zinck, P., & Thielemans, W. (2020). Organocatalyzed ring
484 opening polymerization of lactide from the surface of cellulose nanofibrils. *Carbohydrate Polymers*, 250,
485 116974.

486 Lasseuguette, E. (2008). Grafting onto microfibrils of native cellulose. *Cellulose*, 15(4), 571–580.

487 Lendlein, A., Langer R. (2002). Biodegradable, Elastic Shape-Memory Polymers for Potential Biomedical
488 Applications. *Science*, 296(5573), 1673–1676.

489 Li, C., Sablong, R. J., van Benthem, R. A. T. M., & Koning, C. E. (2017). Unique Base-Initiated
490 Depolymerization of Limonene-Derived Polycarbonates. *ACS Macro Letters*, 6(7), 684–688.

491 Lohmeijer, B. G. G., Pratt, R. C., Leibfarth, F., Logan, J. W., Long, D. A., Dove, A. P., Nederberg, F., Choi,
492 J., Wade, C., Waymouth, R. M., & Hedrick, J. L. (2006). Guanidine and Amidine Organocatalysts for Ring-
493 Opening Polymerization of Cyclic Esters. *Macromolecules*, 39(25), 8574–8583.

494 Marechal, Y., & Chanzy, H. (2000). The hydrogen bond network in Ib cellulose as observed by infrared
495 spectrometry. *Journal of Molecular Structure*, 14.

496 Meimoun, J., Favrelle-Huret, A., Bria, M., Merle, N., Stoclet, G., De Winter, J., Mincheva, R., Raquez, J.-
497 M., & Zinck, P. (2020). Epimerization and chain scission of polylactides in the presence of an organic base,
498 TBD. *Polymer Degradation and Stability*, 181, 109188.

499 Miao, C., & Hamad, W. Y. (2016). In-situ polymerized cellulose nanocrystals (CNC)—poly(l -lactide)
500 (PLLA) nanomaterials and applications in nanocomposite processing. *Carbohydrate Polymers*, 153, 549–
501 558.

502 Nederberg, F., Lohmeijer, B. G. G., Leibfarth, F., Pratt, R. C., Choi, J., Dove, A. P., Waymouth, R. M., &
503 Hedrick, J. L. (2007). Organocatalytic Ring Opening Polymerization of Trimethylene Carbonate.
504 *Biomacromolecules*, 8(1), 153–160.

505 Nyquist, R. A., & Potts, W. J. (1961). Infrared absorptions of organic carbonate derivatives and related
506 compounds. *Spectrochimie Acts*, 17, 679-697.

507 Ottou, W. N., Sardon, H., Mecerreyes, D., Vignolle, J., & Taton, D. (2016). Update and challenges in
508 organo-mediated polymerization reactions. *Progress in Polymer Science*, 56, 64–115.

509 Ottou, W. N., Sardon, H., Mecerreyes, D., Vignolle, J., & Taton, D. (2016). Update and challenges in
510 organo-mediated polymerization reactions. *Progress in Polymer Science*, 56, 64–115.

511 Palard, I., Schappacher, M., Belloncle, B., Soum, A., & Guillaume, S. M. (2007). Unprecedented
512 Polymerization of Trimethylene Carbonate Initiated by a Samarium Borohydride Complex: Mechanistic
513 Insights and Copolymerization with ϵ -Caprolactone. *Chemistry - A European Journal*, 13(5), 1511–1521.

514 Park, S.-A., Eom, Y., Jeon, H., Koo, J. M., Lee, E. S., Jegal, J., Hwang, S. Y., Oh, D. X., & Park, J. (2019).
515 Preparation of synergistically reinforced transparent bio-polycarbonate nanocomposites with highly
516 dispersed cellulose nanocrystals. *Green Chemistry*, 21(19), 5212–5221.

517 Penczek, S., Cypryk, M., Duda, A., Kubisa, P., & Slomkowski, S. (2007). Living ring-opening
518 polymerizations of heterocyclic monomers. *Progress in Polymer Science*, 32(2), 247–28

519 Pendergraph, S. A., Klein, G., Johansson, M. K. G., & Carlmark, A. (2014). Mild and rapid surface initiated
520 ring-opening polymerisation of trimethylene carbonate from cellulose. *RSC Advances*, 4(40), 20737.

521 Revol, J.-F., Bradford, H., Giasson, J., Marchessault, R. H., & Gray, D. G. (1992). Helicoidal self-ordering
522 of cellulose microfibrils in aqueous suspension. *International Journal of Biological Macromolecules*, 14(3),
523 170–172.

524 Sahlin, K., Forsgren, L., Moberg, T., Bernin, D., Rigdahl, M., & Westman, G. (2018). Surface treatment of
525 cellulose nanocrystals (CNC): effects on dispersion rheology. *Cellulose*, 25(1), 331–345.

526 Samuel, C., Chalamet, Y., Boisson, F., Majesté, J.-C., Becquart, F., & Fleury, E. (2014). Highly efficient
527 metal-free organic catalysts to design new Environmentally-friendly starch-based blends. *Journal of*
528 *Polymer Science Part A: Polymer Chemistry*, 52(4), 493–503.

529 Simón, L., & Goodman, J. M. (2007). The Mechanism of TBD-Catalyzed Ring-Opening Polymerization of
530 Cyclic Esters. *The Journal of Organic Chemistry*, 72(25), 9656–9662.

531 Stanley, N., Chenal, T., Jacquel, N., Saint-Loup, R., Prates Ramalho, J. P., & Zinck, P. (2019).
532 Organocatalysts for the Synthesis of Poly(ethylene terephthalate- *co* -isosorbide terephthalate): A Combined
533 Experimental and DFT Study. *Macromolecular Materials and Engineering*, 304(9), 1900298.

534 Thielemans, W., Belgacem, M. N., & Dufresne, A. (2006). Starch Nanocrystals with Large Chain Surface
535 Modifications. *Langmuir*, 22(10), 4804–4810.

536 Trinh, B. M., & Mekonnen, T. (2018). Hydrophobic esterification of cellulose nanocrystals for epoxy
537 reinforcement. *Polymer*, 155, 64–74.

538 Wohlhauser, S., Delepierre, G., Labet, M., Morandi, G., Thielemans, W., Weder, C., & Zoppe, J. O. (2018).
539 Grafting Polymers *from* Cellulose Nanocrystals: Synthesis, Properties, and Applications. *Macromolecules*,
540 *51*(16), 6157–6189.

541 Xu, J., Wu, Z., Wu, Q., & Kuang, Y. (2020). Acetylated cellulose nanocrystals with high-crystallinity
542 obtained by one-step reaction from the traditional acetylation of cellulose. *Carbohydrate Polymers*, *229*,
543 115553.

544 Yao, H., Li, J., Li, N., Wang, K., Li, X., & Wang, J. (2017). Surface Modification of Cardiovascular Stent
545 Material 316L SS with Estradiol-Loaded Poly (trimethylene carbonate) Film for Better Biocompatibility.
546 *Polymers*, *9*(11), 598.

547 Yu, W., E. Maynard, Chiaradia, V., Arno, M.C., Dove, A.P. (2021) Aliphatic Polycarbonates from Cyclic
548 Carbonate Monomers and Their Application as Biomaterials, *Chemical Reviews*, *121*, 10865–10907.

549

550

551